Supplementary Figures and Figure legends

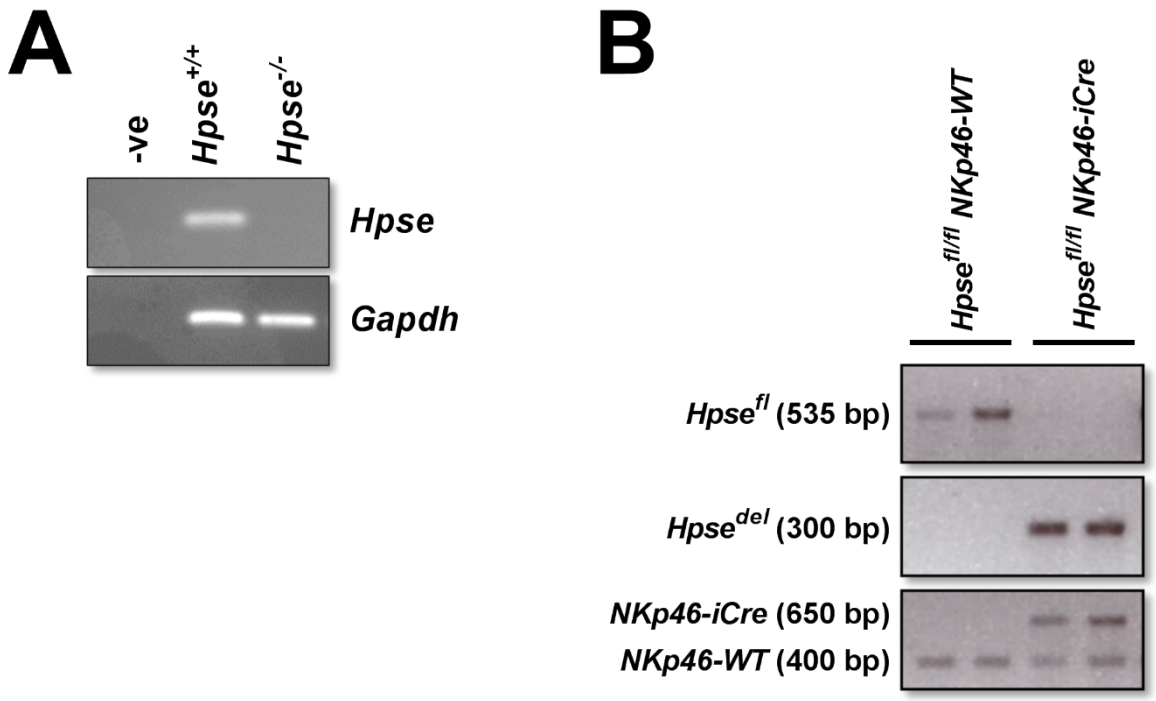

Figure S1: The genetic deletion of heparanase in mouse NK cells. (A) NK cells were purified from spleens of *Hpse*$^{+/+}$ and *Hpse*$^{-/-}$ mice by negative depletion. The expression of *Hpse* mRNA was detected by RT-PCR. The expression of the housekeeping gene *Gapdh* was included as positive control. Data is representative of three independent experiments. (B) *Hpse*$^{fl/fl}$ *NKp46-iCre* mice were generated and the deletion of exon 1 of the *Hpse* gene was examined. PCR detection of various *Hpse* (*Hpse*^{fl} or *Hpse*^{del}) and *NKp46* (*NKp46-WT* or *NKp46-iCre*) alleles was performed in TCRβ^{-}NK1.1^{+}NKp46^{+}DX5^{+} NK cells isolated from *Hpse*$^{fl/fl}$ *NKp46-WT* and *Hpse*$^{fl/fl}$ *NKp46-iCre* mice (n=2; representative of 3 independent experiments).

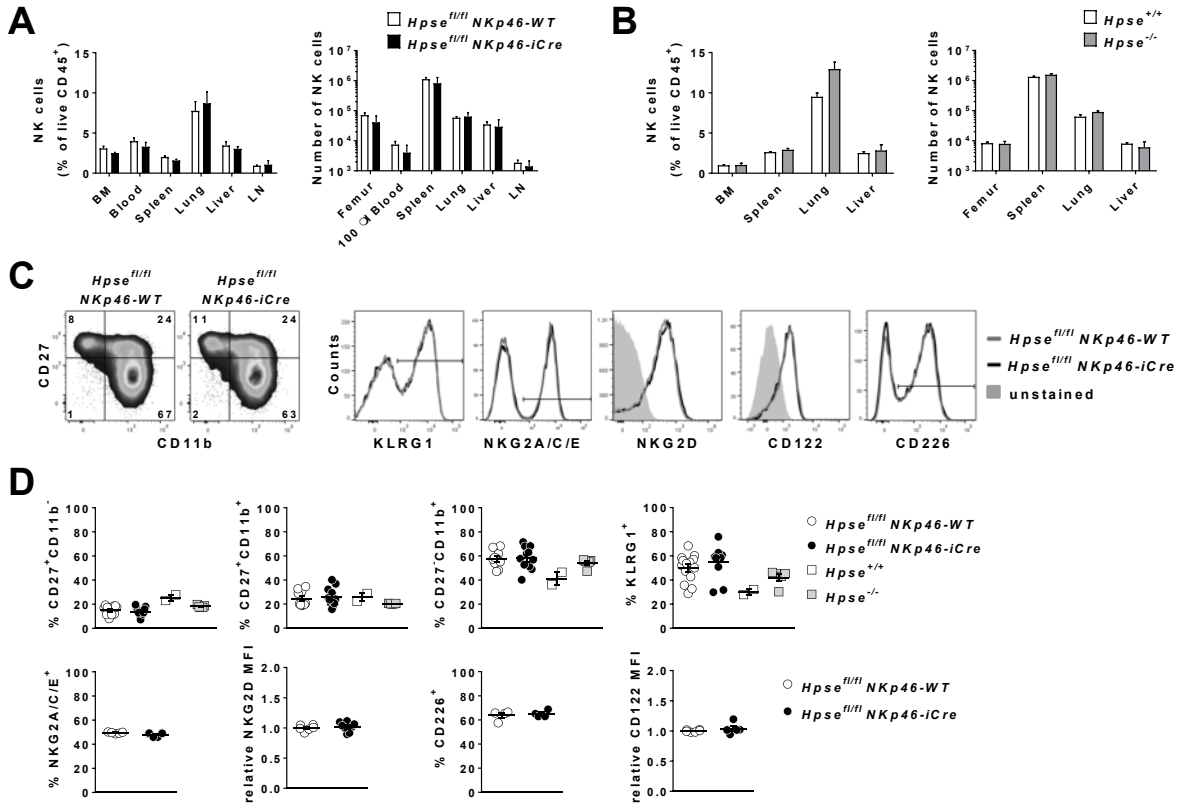

Figure S2: The genetic deletion of heparanase does not affect NK cell numbers or maturation. (A-B) The proportions (left panel) and the absolute numbers of NK cells (right panel) in (A) *Hpse*$^{fl/fl}$ *NKp46-iCre* and *Hpse*$^{fl/fl}$ *NKp46-WT* or (B) *Hpse*$^{+/+}$ and *Hpse*$^{-/-}$ mice were determined by flow cytometry. NK cells were defined as live CD45^{+}TCRβ^{-} NK1.1^{+}NKp46^{+}DX5^{+} (mean ± SEM; A: n=8-9 (BM, blood, lung, liver and lymph node) or n=18-19 (spleen) mice per group; pool of 2-5 independent experiments; B: n=5 (BM, blood, lung, liver, lymph node) or n=2-5 (spleen) mice per group; one representative experiment of two). (C) The expression of maturation markers and surface receptors on splenic NK cells was analysed by flow cytometry. NK cells were defined as live CD45^{+}TCRβ^{-}NK1.1^{+}DX5^{+}. (D) Given are the proportions of NK cells positive for the indicated marker(s) or the relative MFI on NK cells as indicated (mean ± SEM; n=2-14 mice per group; pool of one (CD226), three (KLRG1, CD27/CD11b), or two (all other markers) independent experiments for *Hpse*$^{fl/fl}$ *NKp46-WT* and *Hpse*$^{fl/fl}$ *NKp46-iCre* mice and one experiment for *Hpse*$^{+/+}$ and *Hpse*$^{-/-}$ mice, respectively).

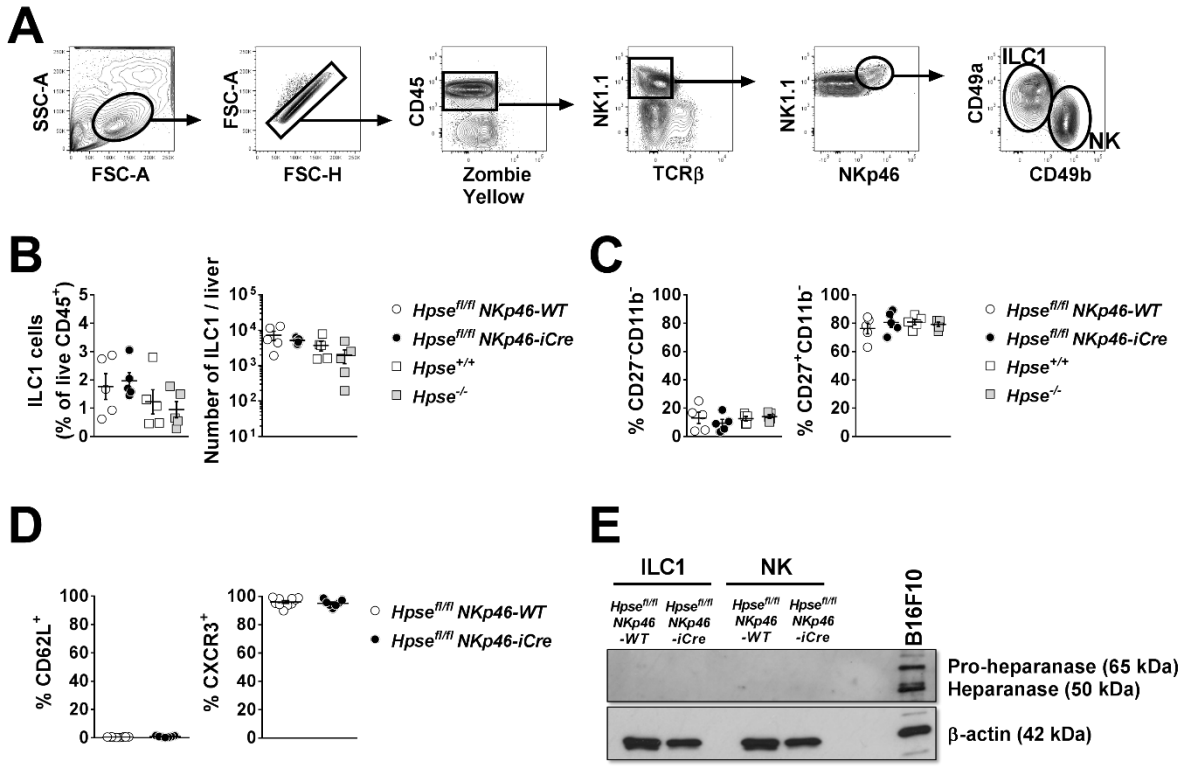

Figure S3: Deletion of heparanase does not affect liver ILC1 cell numbers or phenotype. (A) ILC1 cells were gated as live $CD45^+TCR\beta^-NK1.1^+CD49b^-CD49a^+$ cells, whereas conventional NK cells were gated as $CD45^+TCR\beta^-NK1.1^+CD49b^+CD49a^-$ according to the displayed flow cytometric gating strategy. (B) The proportions (left panel) and absolute numbers (right panel) of ILC1 cells in the liver were determined by flow cytometry (mean ± SEM; n=5 mice per group; one representative experiment of two). The expression of (C) the maturation markers CD27 and CD11b and of (D) the migration marker CD62L and the chemokine receptor CXCR3 on liver ILC1 cells was analysed by flow cytometry (mean ± SEM; n=5-10 mice per group). (E) Hepatic mouse ILC1 cells and conventional NK cells were isolated by FACS sorting and analysed for the expression of heparanase by Western Blotting. Neither ILC1 nor NK cells expressed detectable heparanase levels. B16F10 melanoma cells served as heparanase-positive control and β-actin was used as loading control.

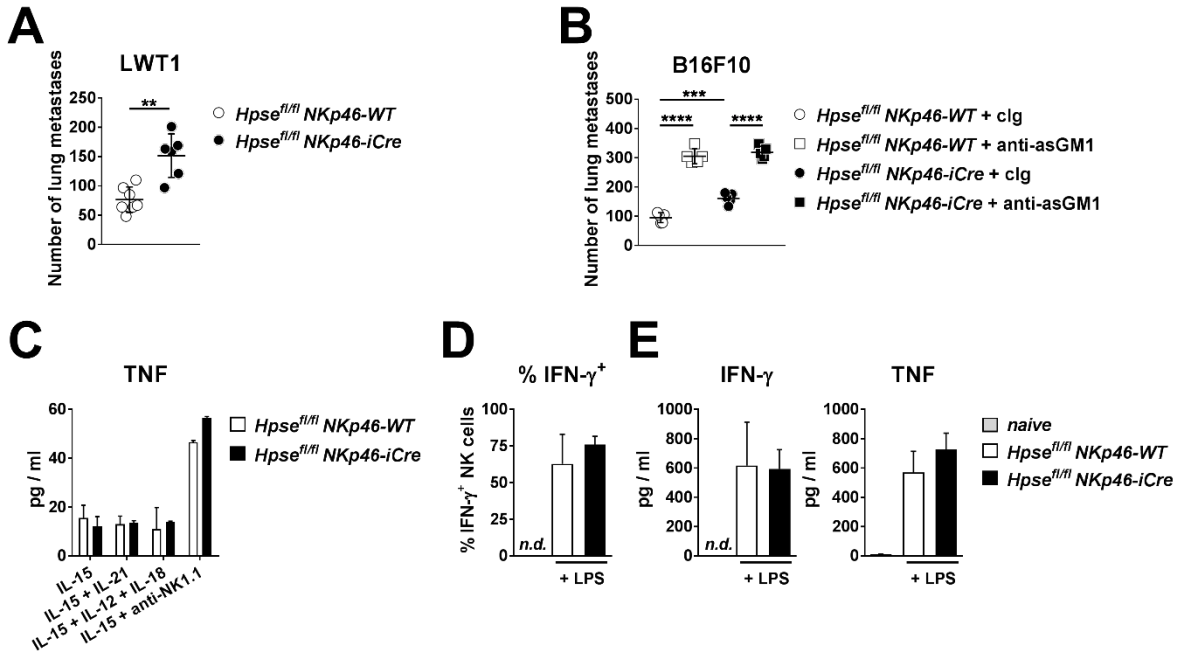

Figure S4: Heparanase-deficiency increases experimental metastasis of the BRAFV600E-mutant melanoma cell line LWT1 but does not affect the capacity of NK cell to produce cytokines. (A) *Hpse*$^{fl/fl}$ *NKp46-WT* and *Hpse*$^{fl/fl}$ *NKp46-iCre* mice were injected i.v. with 2 x 10^5 LWT1 cells. Lungs were harvested on day 14 and macrometastases counted (mean ± SD; n=6-7 mice per group). (B) *Hpse*$^{fl/fl}$ *NKp46-WT* and *Hpse*$^{fl/fl}$ *NKp46-iCre* mice were injected i.v. with 1 x 10^5 B16F10 cells. Mice were injected i.p. with 50 µg control Ig (cIg) or anti-asialo-GM1 (anti-asGM1, NK depletion) on days -1, 0 and 7 relative to tumor inoculation. Lungs were harvested on day 14 and macrometastases counted (mean ± SD; n=5 mice per group). (C) Purified splenic NK cells were stimulated in vitro in the presence of 50 ng/ml IL-15, 100 ng/ml IL-21, 1 ng/ml IL-12, 10 ng/ml IL-18 or anti-NK1.1 pre-coated wells. The release of TNF into the cell culture supernatant was measured after 24 h by CBA (mean ± SD; n=2 biological replicates; one representative experiment of two). (D-E) *Hpse*$^{fl/fl}$ *NKp46-WT* and *Hpse*$^{fl/fl}$ *NKp46-iCre* mice were injected i.p. with 200 µg LPS per 30 g body weight. Naïve mice were used as control (mean ± SEM; n=4; n.d. = not detectable). (D) The expression of IFN-γ in splenic NK cells (gated on $CD45^+TCR\beta^-NK1.1^+NKp46^+DX5^+$) was determined by intracellular staining and flow cytometric analysis. (E) The serum levels of IFN-γ and TNF were determined 6 h after the challenge with LPS by CBA. Statistically significant differences as indicated were determined by (A) Mann-Whitney U test or (B) One-way ANOVA with Tukey's post-test (**: $p < 0.01$; ***: $p < 0.001$; ****: $p < 0.0001$).

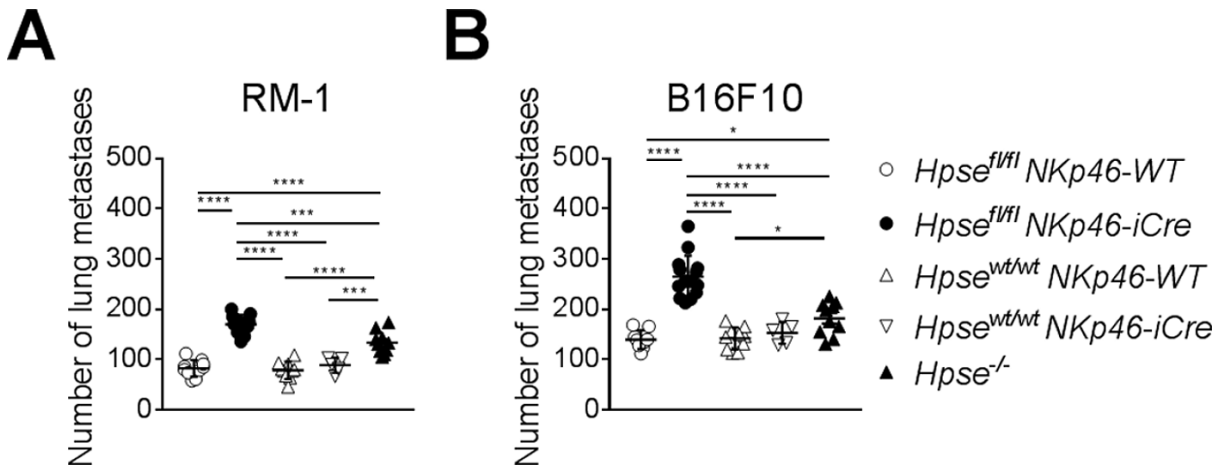

Figure S5: Heparanase-deficient NK cells displayed impaired control of lung metastases. *Hpse*$^{fl/fl}$ *NKp46-WT, Hpse*$^{fl/fl}$ *NKp46-iCre*, *Hpse*$^{wt/wt}$ *NKp46-WT* (B6.WT), *Hpse*$^{wt/wt}$ *NKp46-iCre* and *Hpse*$^{-/-}$ mice were injected i.v. with (A) 1 x 10^5 RM-1 prostate carcinoma cells or (B) 1 x 10^5 B16F10 melanoma cells. Lungs were harvested on day 14 and macrometastases counted (mean ± SEM; n=5-14 mice per group). (A-B) Statistically significant differences between the groups were determined by One-way ANOVA with Tukey's post-test (*: $p<0.05$; ***: $p < 0.001$; ****: $p<0.0001$).

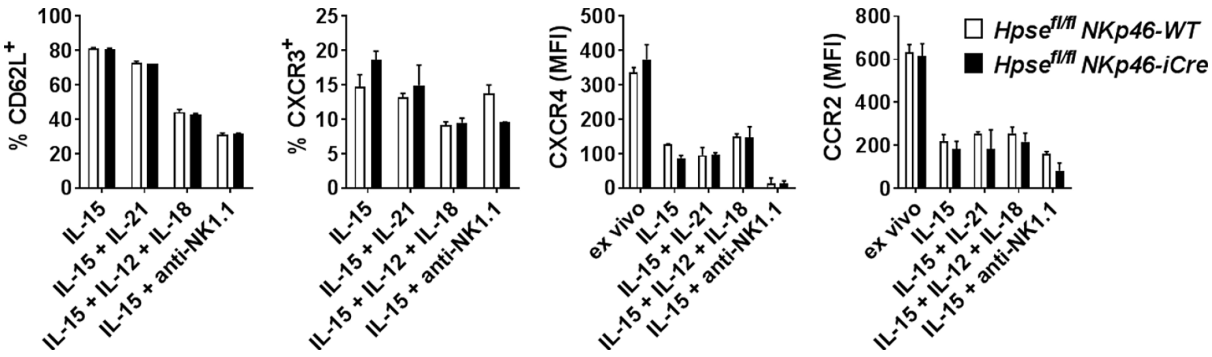

Figure S6: The reduced number of tumor infiltrating NK cells in heparanase-deficient mice is not due to differences in the expression of migration markers and chemokine receptors on NK cells. The expression of migration markers and chemokine receptors on NK cells was determined by flow cytometry. Purified splenic NK cells were stimulated for 24 h in the presence of 50 ng/ml IL-15, 100 ng/ml IL-21, 1 ng/ml IL-12, 10 ng/ml IL-18 or anti-NK1.1 pre-coated wells or analysed ex vivo as indicated (mean ± SEM; n=3-5 (ex vivo) or n=2 biological replicates (in vitro activated)).

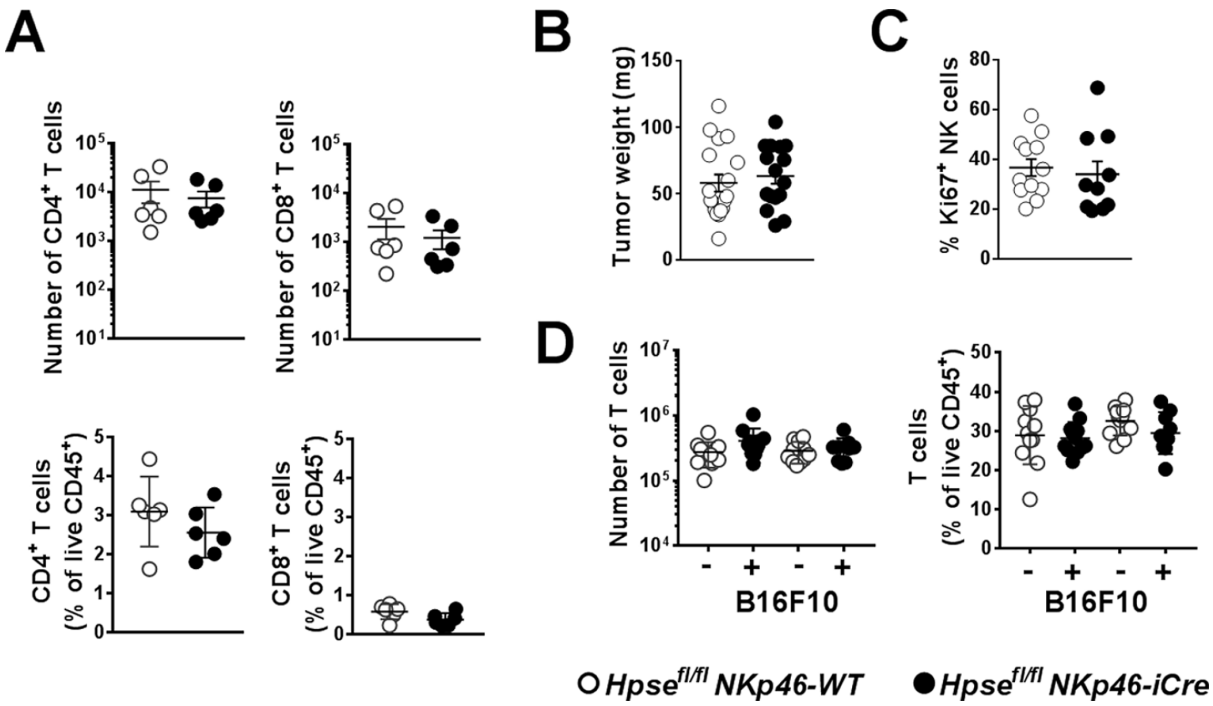

Figure S7: Heparanase-deficiency in NK cells does not affect their proliferation or the infiltration of CD4$^+$ and CD8$^+$ T cells in subcutaneous and metastasis models. (A) *Hpse$^{fl/fl}$ NKp46-WT* and *Hpse$^{fl/fl}$ NKp46-iCre* mice were injected s.c. with 5 x 10^6 RMA-S-Rae1β cells. On day 4, the tumors were harvested and single cell suspensions generated. Samples were stained and the infiltrating lymphocytes were determined as live CD45.2$^+$TCRβ$^+$CD4$^+$ T cells, CD45.2$^+$TCRβ$^+$CD8$^+$ T cells or CD45.2$^+$TCRβ$^-$NK1.1$^+$ NK cells (mean ± SD; n=6 mice per group). (B-C) *Hpse$^{fl/fl}$ NKp46-WT* and *Hpse$^{fl/fl}$ NKp46-iCre* mice were injected s.c. with 5 x 10^6 RMA-S-Rae1β cells and the tumors were harvested on day 4-5. (B) The tumor weight was determined (mean ± SEM; n=16-18 per group, pool of three independent experiments) and (C) the NK cell proliferation was assessed by staining for Ki67 and flow cytometric analysis (mean ± SEM; n=10-12 per group, pool of two independent experiments). (D) *Hpse$^{fl/fl}$ NKp46-WT* and *Hpse$^{fl/fl}$ NKp46-iCre* mice were injected i.v. with 5 x 10^5 B16F10 or PBS control. On day 1, the lungs were harvested and single cell suspensions generated. Samples were stained and the infiltrating T cells were determined as live CD45.2$^+$TCRβ$^+$NK1.1$^-$ cells (mean ± SD; n=9-12 mice per group; pool of 3 independent experiments).